J. Fluid Mech. (1978), *vol.* 88, *part* 2, *pp.* 273–288
Printed in Great Britain

Flow in a channel with pulsating walls

By T. W. SECOMB

Department of Applied Mathematics and Theoretical Physics,
University of Cambridge

(Received 18 November 1977)

In this paper calculations are made of the two-dimensional flow field of an incompressible viscous fluid in a long parallel-sided channel whose walls pulsate in a prescribed way. The study covers all values of the unsteadiness parameter α and the steady-streaming Reynolds number. The wall motion is, in general, assumed to be of small amplitude and sinusoidal. Particular attention is given to the steady component of the flow at second order in the amplitude parameter ϵ. The results for the corresponding problem in axisymmetric geometry are given in an appendix.

Next the following problem is considered: the calculation of the wall motion which will result, in response to prescribed unsteady pressures imposed at the ends of the channel and outside its walls, if the walls are assumed to respond elastically to variations in transmural pressure. It is found that the system has a natural frequency of oscillation, and that resonance will occur if this frequency is close to a multiple of the frequency of the external pressure fluctuations. Finally the preceding work is applied in a discussion of blood flow in the coronary arteries of large mammals.

1. Introduction

A central feature of many physiological flow problems is the distensibility of vessel walls and the wall motion which results under pulsatile flow conditions. The usual approach to such problems is in terms of wave propagation, with the wall displacement dependent on both time and axial distance. Here, however, we consider two model problems in which the wall position depends only on time: two-dimensional flow in a long channel of width $2a(t)$ and axisymmetric flow in a long tube of radius $a(t)$. An important reason for studying these two problems is that the velocity field in each depends linearly on axial distance. This simplifies the equation of motion and makes it possible to find solutions over a wide range of flow parameters (§§ 2–5).

Under physiological conditions the wall motion of a vessel is not usually directly determined by external factors. It is more appropriate to consider the motion as being driven by external *pressures* applied to the ends of a length of vessel and outside its walls. A model problem of this type is investigated in § 6, and the results are applied in § 7 to the flow in the coronary arteries.

Uchida & Aoki (1977) have considered the same problem (in the axisymmetric case) but with a different choice for the function $a(t)$. They showed that if $a(t)$ is a particular *monotonic* function of time then time can be used as a similarity variable, and a solution can be obtained to the full nonlinear equations. The results of the present paper are complementary to theirs.

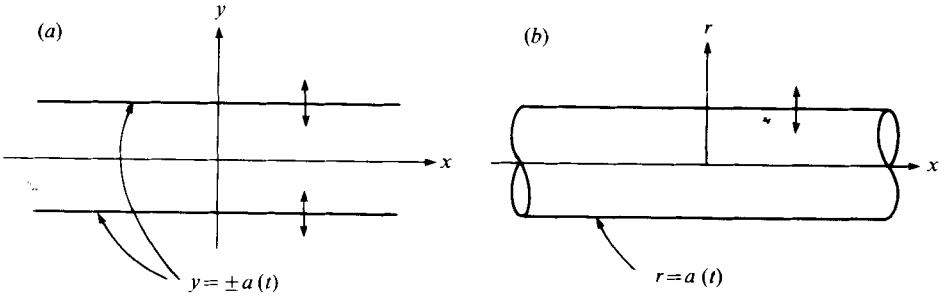

FIGURE 1. The geometry of the two cases to be considered.
(a) Two-dimensional. (b) Axisymmetric.

2. Formulation; solution in the inviscid case

We shall consider the two-dimensional flow of an incompressible fluid in a long channel with rigid walls which move along their normal direction (the y axis) in a prescribed way, so that

$$y = \pm a(t) \quad \text{on the walls.} \tag{2.1}$$

The corresponding problem in cylindrical geometry is that of axisymmetric flow in a long cylinder with radius $r = a(t)$. These two cases are illustrated in figure 1. From here on we consider the two-dimensional case; the corresponding results for the axisymmetric case are summarized in the appendix. Taking velocity components (u, v), the equations of motion are

$$u_t + uu_x + vu_y = -\phi_x + \nu(u_{xx} + u_{yy}), \tag{2.2}$$

$$v_t + uv_x + vv_y = -\phi_y + \nu(v_{xx} + v_{yy}), \tag{2.3}$$

where

$$\phi = p/\rho, \tag{2.4}$$

$$u_x + v_y = 0, \tag{2.5}$$

$$u = 0, \quad v = \pm \dot{a} \quad \text{at} \quad y = \pm a. \tag{2.6}$$

In addition it will prove necessary to make some assumption about the conditions at the ends of the channel to specify the flow completely.

A useful starting point in solving the problem (2.2)–(2.6) is to consider the inviscid problem obtained by dropping the viscous terms in (2.2) and (2.3) and the first, no-slip, condition in (2.6). Assuming a solution for which v is independent of x leads to the general solution

$$u = a\left\{\int \frac{G(t)}{a}\,dt + P(y/a)\right\} - \frac{\dot{a}}{a}x, \tag{2.7}$$

$$v = \dot{a}y/a, \tag{2.8}$$

$$\phi = \phi_c(t) - \tfrac{1}{2}\ddot{a}y^2/a - G(t)\,x + \tfrac{1}{2}(\ddot{a}/a - 2\dot{a}^2/a^2)\,x^2, \tag{2.9}$$

where ϕ_c, G and P are unknown functions. $G(t)$ may be thought of as an externally applied pressure gradient and $P(y/a)$ as the prescribed profile of the flow entering one end of the channel.

A feature of (2.7)–(2.9) is that v is independent of x, u is linear in x, and ϕ is quadratic

in x. We propose that the full viscous solution may have the same structure; accordingly we suppose that

$$(u, v, \phi) = (u_0 + xu_1, v, \phi_0 + x\phi_1 + x^2\phi_2), \tag{2.10}$$

where the unknown functions on the right-hand side are independent of x. If at the same time we scale the y co-ordinate by introducing $\eta = y/a$, so that u_0, u_1, v, ϕ_0, ϕ_1 and ϕ_2 are functions of η and t, we obtain

$$u_{0t} + u_0 u_1 + (v - \dot{a}\eta)\, u_{0\eta}/a = -\phi_1 + \nu u_{0\eta\eta}/a^2, \tag{2.11}$$

$$u_{1t} + u_1^2 + (v - \dot{a}\eta)\, u_{1\eta}/a = -2\phi_2 + \nu u_{1\eta\eta}/a^2, \tag{2.12}$$

$$v_t + (v - \dot{a}\eta)\, v_\eta/a = -\phi_{0\eta}/a + \nu v_{\eta\eta}/a^2, \tag{2.13}$$

$$u_1 + v_\eta/a = 0, \tag{2.14}$$

$$\phi_{1\eta} = 0, \quad \phi_{2\eta} = 0, \tag{2.15), (2.16}$$

$$u_0 = u_1 = 0, \quad v = \pm\dot{a} \quad \text{at} \quad \eta = \pm 1. \tag{2.17}$$

Here (2.12), (2.14) and (2.16) involve only u_1, v and ϕ_2. The quantity u_0 represents a superimposed longitudinal flow. It may be calculated from (2.11) once v has been determined if ϕ_1 is given, along with a suitable condition on the upstream flow profile. However we shall concentrate on the problem for u_1, v and ϕ_2, which is independent of u_0.

3. Solution for small α

We define the unsteadiness parameter (Womersley number) α by

$$\alpha = a_0(\omega/\nu)^{\frac{1}{2}}, \tag{3.1}$$

where ν is the kinematic viscosity, ω is a characteristic frequency of the wall oscillations and a_0 is a typical half-width or radius of the channel or tube. When α is small we may solve the problem in powers of α^2 when $a(t)$ is an arbitrary function of time. Writing (2.12) in the form

$$u_{1\eta\eta} = g + \alpha^2(a^2 u_{1t} + a^2 u_1^2 + a(v - \dot{a}\eta)\, u_{1\eta})/(\omega a_0^2), \tag{3.2}$$

where

$$g(t) = 2\alpha^2 a^2 \phi_2/(\omega a_0^2),$$

we find that

$$u_1 = \tfrac{3}{2}(\dot{a}/a)(\eta^2 - 1) + \alpha^2[\tfrac{1}{40} a\ddot{a}(\eta^2 - 1)(5\eta^2 - 1) + \tfrac{1}{2\,80}\dot{a}^2(\eta^2 - 1)(7\eta^4 - 98\eta^2 + 19)]/(\omega a_0^2) + O(\alpha^4\omega), \tag{3.3}$$

$$v = \tfrac{1}{2}\dot{a}\eta(3 - \eta^2) - \alpha^2[\tfrac{1}{40} a^2\ddot{a}\eta(\eta^2 - 1)^2 + \tfrac{1}{2\,80} a\dot{a}^2\eta(\eta^2 - 1)^2(\eta^2 - 19)]/(\omega a_0^2) + O(\alpha^4\omega a_0), \tag{3.4}$$

$$\phi_2 = \tfrac{3}{2}\alpha^{-2}\omega a_0^2 \dot{a}/a^3 + (\tfrac{3}{5}\ddot{a}/a - \tfrac{51}{35}\dot{a}^2/a^2) + O(\alpha^2\omega^2). \tag{3.5}$$

We see that the pressure is dominated by a viscous term depending on $\dot{a}$, and that inertial effects only appear at the next order.

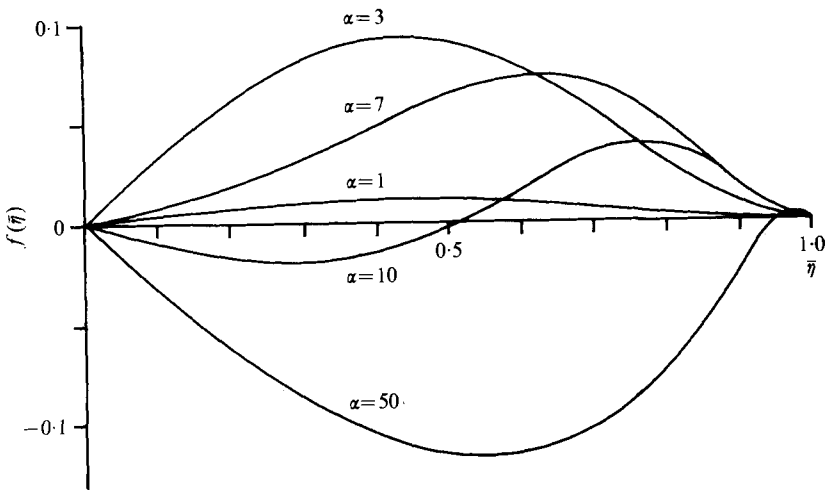

FIGURE 2. The Lagrangian mean streaming velocity in two-dimensional geometry [equation (4.10)].

4. Solution for arbitrary α and small sinusoidal wall displacements

In this section we assume that $\alpha > 0$ and that the wall motion takes the form

$$a(t) = a_0(1 + \epsilon \cos \omega t) \quad \text{where} \quad \epsilon \ll 1. \tag{4.1}$$

We produce a solution as a power series in ϵ up to second order. If we consider the form of the problem for u_1, v and ϕ_2 and the effect of changing the sign of ϵ, we see that the solution must take the form

$$\phi_2 = \epsilon \,\mathrm{Re}\,(\phi_2^{[11]} e^{i\omega t}) + \epsilon^2[\phi_2^{[20]} + \mathrm{Re}\,(\phi_2^{[22]} e^{2i\omega t})] + O(\epsilon^3), \tag{4.2}$$

and similarly for u_1 and v, where the quantities $\phi_2^{[ij]}$ are independent of time and represent the jth Fourier component of the ith-order term in the expansion of the quantity ϕ_2. In § 5 we shall discuss the convergence properties of this series in ϵ.

First-order solution. Equations (2.12), (2.14) and (2.17) give at first order in ϵ

$$i\omega u_1^{[11]} = -2\phi_2^{[11]} + \nu a_0^{-2} u_{1\eta\eta}^{[11]},$$

$$u_1^{[11]} + a_0^{-1} v_\eta^{[11]} = 0,$$

$$v^{[11]} = \pm i\omega a_0, \quad u_1^{[11]} = 0 \quad \text{at} \quad \eta = \pm 1.$$

This has the solution

$$\phi_2^{[11]} = -\tfrac{1}{2}\omega^2 \cosh \beta / D, \tag{4.3}$$

$$u_1^{[11]} = -i\omega(\cosh \beta - \cosh \beta\eta)/D, \tag{4.4}$$

$$v^{[11]} = i a_0 \omega(\eta \cosh \beta - \sinh \beta\eta/\beta)/D, \tag{4.5}$$

where $$\beta = \alpha e^{\frac{1}{4}i\pi}, \quad D = \cosh \beta - \sinh \beta/\beta.$$

Second-order solution, steady component. Here we find that

$$\nu a_0^{-2} u_{1\eta\eta}^{[20]} - 2\phi_2^{[20]} = \tfrac{1}{4}[-(\nu/a^2)^{[11]*} u_{1\eta\eta}^{[11]} + u_1^{[11]} u_1^{[11]*} + (\nu/a - \dot{a}\eta/a)^{[11]} u_{1\eta}^{[11]*}] + \text{c.c.} \tag{4.6}$$

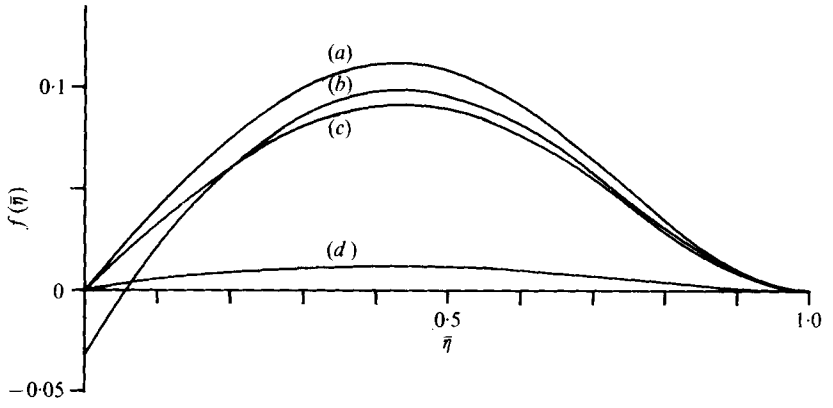

FIGURE 3. Comparison of exact and approximate formulae for the Lagrangian mean streaming velocity in two-dimensional geometry. (*a*) $\alpha = 3$, small α result from (3.4). (*b*) $\alpha = 3$, large α result (5.3). (*c*) $\alpha = 3$, arbitrary α result (4.10). (*d*) $\alpha = 1$, results of (3.4) and (4.10) agree almost exactly.

and

$$u_1^{[20]} + a_0^{-1} v_\eta^{[20]} = -\tfrac{1}{4}(1/a)^{[11]*} v_\eta^{[11]} + \text{c.c.}, \tag{4.7}$$

where an asterisk and c.c. denote the complex conjugate, subject to

$$v^{[20]} = u_1^{[20]} = 0 \quad \text{at} \quad \eta = \pm 1. \tag{4.8}$$

These equations are solved to obtain $\phi_2^{[20]}$, $u_1^{[20]}$ and $v^{[20]}$. Of more direct interest, however, is the Lagrangian mean velocity field, since this gives the actual drift of material particles. To obtain this we first calculate the Eulerian velocity field, by expressing the velocity field already calculated in terms of the steady co-ordinate y rather than the time-dependent co-ordinate η. We then calculate the Lagrangian mean velocity $\mathbf{u}_L$ at second order through the relation

$$\mathbf{u}_L = \mathbf{u}_E + \langle \int \mathbf{v}\, dt . \nabla \mathbf{v} \rangle,$$

where $\mathbf{u}_E$ is the steady second-order component of the Eulerian velocity, $\mathbf{v}$ is the velocity at first order and the angle brackets denote a time average. We obtain

$$v_L = \omega a_0 f(\bar{\eta}), \quad u_{1L} = -\omega f'(\bar{\eta}), \tag{4.9}$$

where

$$\bar{\eta} = y/a_0$$

and

$$f(\bar{\eta}) = \frac{1}{4DD^*}\left[\tfrac{3}{4}(\cosh 2^{\frac{1}{2}}\alpha - \cos 2^{\frac{1}{2}}\alpha)(\bar{\eta}^3 - \bar{\eta}) + \frac{11}{2^{\frac{5}{2}}\alpha}(\sinh 2^{\frac{1}{2}}\alpha - \sin 2^{\frac{1}{2}}\alpha)(3\bar{\eta} - \bar{\eta}^3)\right.$$
$$\left. - \frac{3}{2^{\frac{3}{2}}\alpha}(\sinh 2^{\frac{1}{2}}\alpha\bar{\eta} - \sin 2^{\frac{1}{2}}\alpha\bar{\eta}) - \left(\frac{4}{\beta^*}\sinh\beta\bar{\eta}\cosh\beta^* + \text{c.c.}\right)\right]. \tag{4.10}$$

The function $f(\bar{\eta})$ is plotted in figure 2 for several values of α. It is especially interesting to notice the reversal of the flow at large α, compared with small α, in the interior of the channel. At small α the Lagrangian mean velocity is directed towards the wall, while at large α it is away from the wall except in a thin boundary layer at the wall. When $\alpha \lesssim 1$, (4.10) is found to agree very closely with the form of v_L deduced from (3.4); see figure 3. The leading term is then of order α^2.

Second-order solution, oscillatory component. This can be calculated in a similar way; however we omit it here.

5. Solution for large α; importance of steady-streaming Reynolds number

We now examine the possible range of validity of our power-series solution, considered as an asymptotic expansion. We assume that the behaviour of the first few terms is indicative. When $\alpha \lesssim 1$ the results of § 3 may be used to obtain estimates for the first few terms of the power series in ϵ. These are easily seen to be well behaved, and we conclude that the solution given in § 4 is a valid expansion for $\epsilon \ll 1$ and $\alpha \lesssim 1$.

In order to exhibit the form of this solution when α is large, we give the following approximations, under the rather mild assumption that $\exp(-\alpha/2^{\frac{1}{2}}) \ll 1$:

$$\phi_2^{[11]} \cong -\frac{1}{2}\frac{\omega^2}{1-1/\beta}; \tag{5.1}$$

$$v^{[11]} \cong ia_0\omega\frac{\eta-\exp\{-\beta(1-\eta)\}/\beta}{1-1/\beta}; \tag{5.2}$$

$$v_L \cong \frac{\frac{1}{4}a_0\omega}{1-2^{\frac{1}{2}}/\alpha+1/\alpha^2}\left[\tfrac{3}{2}(\bar{\eta}^3-\bar{\eta})+\frac{11}{2^{\frac{3}{2}}\alpha}(3\bar{\eta}-\bar{\eta}^3)-\frac{3}{2^{\frac{1}{2}}\alpha}\exp\{-2^{\frac{1}{2}}\alpha(1-\bar{\eta})\}\right.$$
$$\left.-\left(\frac{4}{\beta^*}\exp\{-\beta(1-\bar{\eta})\}+\text{c.c.}\right)\right]; \tag{5.3}$$

i.e.
$$v_L = \tfrac{3}{8}a_0\omega[\bar{\eta}^3-\bar{\eta}+O(\alpha^{-1})+\text{exponential terms}]. \tag{5.4}$$

These results turn out to be good approximations to the results of § 4 when $\alpha \gtrsim 3$; see figure 3. Apart from a multiplicative constant, the velocity at first order is seen to comprise the inviscid solution $v^{[11]} = ia_0\omega\eta$ modified by an exponential term representing a Stokes-type oscillatory boundary layer. In (5.4) we see that the dominant term in the Lagrangian mean velocity v_L is independent of α and represents the flow in the core driven by the steady velocity $-\frac{3}{4}\epsilon^2\omega x$ which is induced at the edge of the Stokes layer (see Batchelor 1967, p. 360). Rayleigh (1884) obtained the same y dependence for the steady streaming induced by a standing sound wave between parallel plates.

If the calculation is extended to fourth order in ϵ, with the assumption that α is large, it is found that $u_1^{[40]} = O(\alpha^2)$ whereas $u_1^{[20]} = O(1)$ as $\alpha \to \infty$. Therefore we should not expect the series to be valid as an asymptotic representation unless $\epsilon^2\alpha^2$ is small. Indeed, returning to (4.6), we see that the viscous term $\epsilon^2\nu a_0^{-2}u_{1\eta\eta}^{[20]}$ was included while convective terms such as $\epsilon^4 u_{1\eta}^{[20]2}$ were neglected. The ratio of the former to the latter in the core is of magnitude $R_s = \epsilon^2\alpha^2$, the steady-streaming Reynolds number (Stuart 1963), and we see that the results obtained so far are valid only if $R_s \ll 1$.

We now give an alternative approach valid for $R_s \geqslant O(1)$ and large α. From (2.12) and (2.14) we have

$$v_{\eta t}-\dot{a}v_\eta/a-v_\eta^2/a+(v-\dot{a}\eta)v_{\eta\eta}/a = 2a\phi_2+\nu v_{\eta\eta\eta}/a^2.$$

In order to simplify the nonlinear terms, we suppose that

$$v(\eta,t) = \dot{a}\eta+a^3F(\eta,t). \tag{5.5}$$

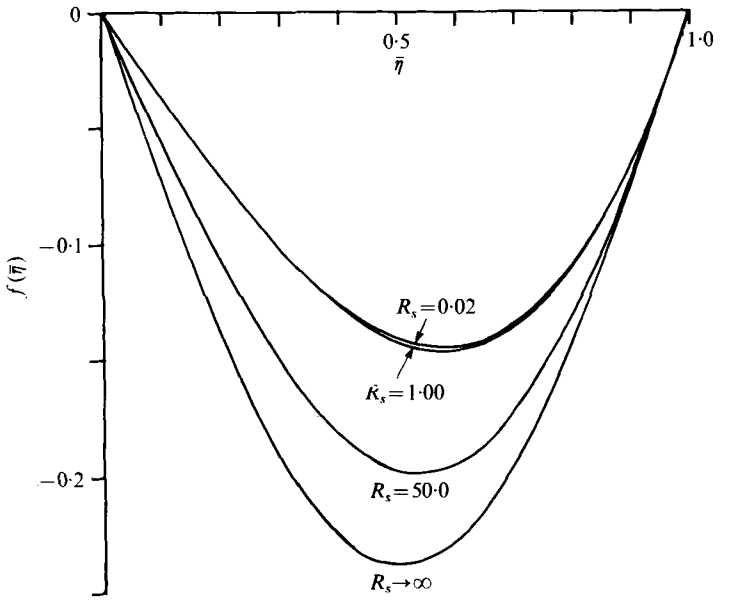

FIGURE 4. The steady streaming velocity in the core in two-dimensional geometry for large α, from (5.9) (R_s finite) and (5.16) ($R_s \to \infty$).

This gives

$$F_{\eta t} + a^2(FF_{\eta\eta} - F_\eta^2) = 2\bar{\phi}_2/a^2 + \nu F_{\eta\eta\eta}/a^2, \tag{5.6}$$

where

$$\bar{\phi}_2 = \phi_2 - \tfrac{1}{2}\ddot{a}/a + \dot{a}^2/a^2,$$

subject to

$$F = 0, \quad F_\eta = -\dot{a}/a^3 \quad \text{at} \quad \eta = \pm 1. \tag{5.7}$$

The problem (5.6) and (5.7) was solved by the method of matched asymptotic expansions for the following two cases:

(i) $\alpha = N\epsilon^{-1}$, so that $R_s = N^2 = O(1)$ as $\epsilon \to 0$;

(ii) $\alpha = N\epsilon^{-1-c}$, where $c > 0$, so that $R_s \to \infty$ as $\epsilon \to 0$.

We omit the details of the solution. In each case the matching of the core solution to the boundary-layer solution gives rise to the following boundary conditions on the flow in the core:

$$F^{[20]}(\pm 1) = 0, \quad F_\eta^{[20]}(\pm 1) = \tfrac{3}{4}\omega a_0^{-2}. \tag{5.8}$$

(These are, in effect, the same as the boundary conditions satisfied by the low R_s solution (5.4) outside the boundary layer.) Within the core the function F is found to vanish at first order, so that the Lagrangian and Eulerian mean velocities coincide and are given by

$$v_L = a_0^3 F^{[20]} = a_0 \omega f(\eta),$$

where $f(\eta)$ satisfies

$$\text{(i)}\ f''' = N^2(ff'' - f'^2 - K) \tag{5.9}$$

or

$$\text{(ii)}\ ff'' - f'^2 = K, \tag{5.10}$$

subject in each case to

$$f(\pm 1) = 0, \quad f'(\pm 1) = \tfrac{3}{4}, \tag{5.11}$$

where K is a constant. (We see that the steady flow to this order is not modified in the core by interaction with the oscillatory flow. In general this point does not appear to be trivial. See, for example, Stuart 1966.)

The problem (5.9) and (5.11) was solved numerically; figure 4 shows the results for several values of R_s. Equation (5.10) arises also from a problem studied by Proudman (1960). Proudman investigated the conditions under which a solution of (5.10) can be the limit as $N \to \infty$ of solutions of (5.9). He showed that, apart from the linear solution which satisfies (5.10) and (5.9) exactly, any solution of (5.10) with a zero at which $f' < 0$ must be the limit of a sequence of solutions of (5.9) in which there is a rapid transition in a third or higher derivative at the zero. A solution with a zero at which $f' > 0$ cannot be the limit of a sequence of solutions of (5.9).

In this case, we use Proudman's result to remove the ambiguity in the solution of (5.10) and (5.11), which have a family of solutions

$$f_n(\eta) = -\frac{3(-1)^n}{4n\pi} \sin n\pi\eta, \quad n = 1, 2, 3, \ldots. \tag{5.12}$$

Of these we see that only f_1 has no zeros in the interior with $f' > 0$, so we conclude that the appropriate solution is

$$f(\eta) = -\tfrac{3}{4}\pi^{-1} \sin \pi\eta. \tag{5.13}$$

The changes in the core steady streaming with R_s are shown in figure 4. Notice that the flow in the limit $R_s \to 0$ coincides with the limit as $\alpha \to \infty$ of the core flow at small R_s shown in figure 2. In the limit $R_s \to \infty$, the solution of (5.9) should approach (5.13). This trend may be seen in figure 4; however, to obtain close agreement a very large value of $N^2 = R_s$ would be required, which would make (5.9) awkward for computation.

Previous studies of the steady streaming driven by a Stokes-type boundary layer at large R_s have mainly concerned exterior flows. Riley (1967) reviewed earlier work on the subject and showed how the problem of calculating the steady flow driven by an oscillating body may be formulated in terms of matched asymptotic expansions under several different conditions on the parameters ϵ, α and R_s. The particular case of a cylinder oscillating along a diameter in an unbounded fluid at large R_s has been considered by Riley (1965) and by Stuart (1966). They showed that, near the points on the surface of the cylinder at the $\pm \frac{1}{2}\pi$ positions with respect to the direction of oscillation, the oscillatory boundary layer drives a steady flow which is directed *away* from these points, and that this produces a second boundary layer of thickness of order $a_0 R_s^{-\frac{1}{2}}$, where a_0 is a characteristic length.

In the present case, however, the oscillatory boundary layer drives a steady flow which is directed *inwards*, towards the point $x = 0$ (neglecting the independent component u_0 of the velocity). This fact is implied by (5.8). Physically, we should not expect the vorticity generated by the oscillatory layer to be confined to a second boundary layer when advection is leading to a concentration of vorticity, and indeed it can be shown that there can be no steady boundary-layer-type flow driven by such a steady velocity at the edge of the oscillatory layer. In Stuart's (1966) problem a similar situation arises near the points where the surface of the cylinder meets the diameter in the direction of oscillation. He suggested a jet-like solution in which

vorticity is continually carried away from the cylinder. On the other hand, Longuet-Higgins (1953) suggested that the steady streaming at large values of R_s can in some cases be calculated by the theory of inviscid rotational flow. Here we have given an example which suggests that when the steady velocity at the edge of the oscillatory layer is directed '*inwards*' in a *confined* flow, an inviscid rotational streaming takes place throughout the flow domain.

6. Elastically constrained walls

In this section we consider a channel of finite length located on the interval

$$A \leqslant x \leqslant B,$$

where $L = B - A \gg a_0$. Its ends are supposed to be joined to reservoirs of fluid at pressures $\rho\phi_A(t)$ and $\rho\phi_B(t)$ respectively, while the pressure outside the walls is $\rho\phi_E(t)$. We assume as before that the walls remain parallel, occupying the positions $y = \pm a(t)$. As we intend this model to represent a portion of an artery, we introduce an elastic constraint on the motion of the walls of the form

$$p_{TMA} = \rho f(a) \quad \text{with} \quad f(a_0) = 0, \tag{6.1}$$

where p_{TMA} is the pressure difference across the wall averaged along the channel. In imposing this relation we are implicitly neglecting the wall mass and internal wall friction.

Before applying the results of the previous sections to this problem, we need to consider what modifications they require when the channel has finite length. Let us suppose, for example, that the x-independent flow component u_0 has a steady part of order $u_0^{(s)}$ and an oscillating part with magnitude of order $u_0^{(u)}$ and frequency ω. To leading order the corresponding quantities for the x-dependent component u_1 are $u_1^{(s)} = \epsilon^2\omega L$ and $u_1^{(u)} = \epsilon\omega L$ at the ends of the channel. We shall estimate the 'entry length' l for each of these four components on the assumption that they may be treated independently. For the two oscillating components, we use the maximum displacement of a fluid element during one cycle as our estimate, obtaining

$$l_0^{(u)} = 2\omega^{-1}u_0^{(u)} \quad \text{and} \quad l_1^{(u)} = 2\epsilon L.$$

For the two steady components, the entry length is of the order ka_0R, where R is the Reynolds number and k a small constant ($k \simeq 0{\cdot}06$ for Poiseuille flow developing from a blunt profile in a tube). Thus $l_0^{(s)} = k_0\alpha^2\omega^{-1}u_0^{(s)}$ and $l_1^{(s)} = k_1R_sL$, where k_0 an k_1 are unknown constants. For a given u_0, we see that if L is sufficiently large $l_0^{(s)}$, $l_0^{(u)} \ll L$. Since $\epsilon \ll 1$, $l_1^{(u)} \ll L$. However, we see that if R_s is large $l_1^{(s)}$ may be of order L or greater, and so 'end' effects modifying the steady streaming may in fact persist throughout the whole length of the channel. In this section we are primarily concerned with the oscillating components of the pressure field, so this effect may not be important. If R_s is order unity or smaller, then $l_1^{(s)} \ll L$.

We shall assume that end effects will have a negligible effect on any average taken over the length of the channel. We also neglect transverse pressure variation. From (6.1) we obtain

$$L^{-1}\int_A^B (\phi_0 + x\phi_1 + x^2\phi_2)\,dx - \phi_E = f(a)$$

and the end conditions are that

$$\phi_A = \phi_0 + A\phi_1 + A^2\phi_2$$

and similarly at $x = B$. We deduce that

$$\tfrac{1}{6}L^2\phi_2 + f(a) = \phi_F, \tag{6.2}$$

where

$$\phi_F = \tfrac{1}{2}(\phi_A + \phi_B) - \phi_E. \tag{6.3}$$

First we consider the inviscid problem. We have seen in §§ 4 and 5 that the flow in the limit of small viscosity is not the inviscid flow: in particular, the inviscid flow contains no steady streaming. However we find that in the large R_s problem the quantity $\overline{\phi}_2$, representing the deviation from the inviscid pressure, vanishes to at least second order in the amplitude parameter ϵ, so the inviscid form of ϕ_2 may be expected to be a good approximation at large R_s, even for non-sinusoidal wall motion. In the inviscid case, (6.2) gives

$$\ddot{a}/a - 2\dot{a}^2/a^2 + 12f(a)/L^2 = 12\phi_F/L^2. \tag{6.4}$$

With the substitution $s = a_0/a$, this becomes

$$\ddot{s} - 12sf(a_0/s)/L^2 = -12\phi_F s/L^2. \tag{6.5}$$

Let us now assume a linear approximation to $f(a)$ and a sinusoidal pressure disturbance

$$f(a) = k(a - a_0), \quad \phi_F = A_F \cos\omega t.$$

If we set $\kappa^2 = 12ka_0/L^2$ and $\mu = 12A_F/L^2$ we obtain

$$\ddot{s} + (\kappa^2 + \mu\cos\omega t)\, s = \kappa^2. \tag{6.6}$$

Equation (6.6) is a slight variation of the well-known Mathieu equation

$$d^2u/dz^2 + (p - 2q\cos 2z)\, u = 0. \tag{6.7}$$

The behaviour of the solutions of (6.7) is governed by the parameters p and q (see Abramowitz & Stegun 1965, p. 724). A set of characteristic curves, on each of which (6.7) has periodic solutions of period 2π, divides the p, q plane into regions of two types: regions (containing the p axis) where (6.7) has two independent bounded solutions and regions where (6.7) has an unbounded solution.

To complete the solution of (6.6) we have to find a particular solution. Putting $z = \frac{1}{2}\omega t$, $p = 4\kappa^2/\omega^2$ and $q = -2\mu/\omega^2$ we have

$$d^2s/dz^2 + (p - 2q\cos 2z)\, s = p. \tag{6.8}$$

A particular solution may be obtained by expanding p and s in powers of q about a known periodic solution for $q = 0$. For instance if we assume

$$s = 1 + C\cos 2z + O(q), \quad p = 4 + O(q),$$

where s is periodic, we obtain

$$s = 1 + C\cos 2z + (\tfrac{1}{4} - \tfrac{1}{12}\cos 4z)\, q + \ldots, \tag{6.9}$$

$$p = 4 + 2C^{-1}q + \tfrac{5}{12}q^2 - \tfrac{19}{72}C^{-1}q^3 - \tfrac{1}{27}(\tfrac{763}{512} - \tfrac{53}{16}C^{-1})\, q^4 + \ldots. \tag{6.10}$$

Omitting for a moment the terms of (6.10) containing the factor C^{-1}, we are left with the formula for one of the characteristic curves. Hence if the point (p, q) lies close to

this curve, a periodic particular solution will exist with large amplitude C. Such a resonance occurs whenever $p = 4n^2 + O(q)$, i.e. whenever $\kappa \cong n\omega$. Note however that an unbounded solution may be superimposed on this particular solution if (p, q) lies in an unstable region. In practice there must be some viscous damping present which will limit the amplitude of the motion. An order-of-magnitude calculation based on energy dissipation in the boundary layer suggests that the amplitude of the motion has an upper bound a_m given by

$$a_m/a_0 \sim (kA_F/\omega^2 L^2)\,\alpha \quad \text{as} \quad \alpha \to \infty, \tag{6.11}$$

where k is a constant. This estimate is independent of the steady-streaming Reynolds number.

We can be more precise about the effect of viscosity if we assume small wall motion and small R_s, so that the analysis of § 4 is relevant. If we assume that $\exp(-\alpha/2^{\frac{1}{2}}) \ll 1$ and that

$$a(t) = a_0\{1 + \epsilon\alpha_1 \cos\omega t + \epsilon^2[\mathrm{Re}\,(\alpha_2 e^{2i\omega t}) + \text{constant}] + O(\epsilon^3)\},$$

we find that

$$\phi_2^{[11]} = -\tfrac{1}{2}\alpha_1 \frac{\omega^2}{1 - 1/\beta} \quad (\text{where } \beta = \alpha e^{\frac{1}{4}i\pi})$$

and

$$\phi_2^{[22]} = \omega^2 \left[\frac{-2\alpha_2}{1 - 1/(2^{\frac{1}{2}}\beta)} + \alpha_1^2(\tfrac{3}{4} + O(\alpha^{-2}))\right].$$

Assume now that $\phi_F = \phi_F^{[11]} \cos\omega t$ and that (6.2) holds. Using a Taylor-series expansion for $f(a)$, we obtain

$$\alpha_1 = \frac{12\phi_F^{[11]}/L^2}{\kappa^2 - \omega^2/(1 - 1/\beta)} \quad (\text{where } \kappa^2 = 12a_0 f'(a_0)/L^2) \tag{6.12}$$

and

$$\alpha_2 = -\alpha_1^2 \frac{3a_0^2 f''(a_0)/L^2 + (\frac{3}{2} + O(\alpha^{-2}))\,\omega^2}{\kappa^2 - 4\omega^2/[1 - 1/(2^{\frac{1}{2}}\beta)]}. \tag{6.13}$$

Suppose that $\phi_F^{[11]}$ is kept fixed but ω is varied. Then we see from (6.12) that a resonance peak in $|\alpha_1|$ will occur near $\omega = \kappa$. In fact, to a good approximation the maximum value of $|\alpha_1|$ occurs when the denominator is pure imaginary, and is given by

$$|\alpha_1| = 12 \times 2^{\frac{1}{2}}\alpha |\phi_F^{[11]}| \omega^{-2} L^{-2}(1 + O(\alpha^{-1})).$$

This is consistent with (6.11). Equation (6.13) shows that another resonance will occur at $\omega \cong \frac{1}{2}\kappa$, even if the function $f(a)$ is linear. The further resonances found in the inviscid case could be demonstrated by carrying the calculation to higher orders.

7. Application to coronary flow

The coronary arteries differ from other arteries in that they run for much of their length within the muscular wall of the heart and thus are subjected to a varying external pressure. This pressure is greatest during the ejection phase of the cardiac cycle (systole), and it is observed that the coronary flow has a minimum during systole, suggesting that the external pressure is sufficient to reduce significantly the vessel cross-section. If this constriction is assumed to be uniform along the length of the vessel, a situation similar to our model problem results. The axisymmetric case is perhaps the more appropriate.

Another particular feature of coronary blood flow, especially in large animals such as horses and large dogs, is the presence of fluctuations in the flow velocities, with frequencies of from 5 to 10 Hz. These have been found by several authors in open-chest measurements on anaesthetized animals (Rumberger & Nerem 1977; Nerem *et al.* 1976; Wells *et al.* 1974). Tentative explanations have been put forward, such as wave reflexion or the presence of elastic waves in the heart wall. Rumberger & Nerem were able to reproduce the effect in a computer simulation of a coronary artery without, however, deducing any basic mechanism for the oscillations.

In this section we show that the model problem we have studied allows for oscillations in the same frequency range, and can therefore give some insight into a possible mechanism for the *in vivo* oscillations. We saw in § 6 that in our model, as long as viscosity is not too large, the wall has a natural frequency of oscillation given (in the axisymmetric case) by (A 17) (see appendix). To obtain an estimate for the elastic constant $a_0 f'(a_0)$ we use Rumberger & Nerem's (1977) measurements of the wave propagation velocity c in the left anterior descending coronary artery of the horse. They found that the velocity is strongly dependent on the intraluminal pressure and on the distance along the artery. A typical value is of the order of $c_0 = 8\,\mathrm{m/s}$. The vessel length, following a major branch, is about 50 cm. By standard theory, $c = (\rho D)^{-\frac{1}{2}}$, where the distensibility D is given by

$$D = A^{-1} dA/dp = 2(\rho a f'(a))^{-1}$$

and $A = \pi a^2$ is the cross-sectional area. To the present approximation,

$$c_0^2 = (\rho D)^{-1} = \tfrac{1}{2} a_0 f'(a_0),$$

and from (A 17), $\kappa = 2 \times 3\frac{1}{2} c_0/L$. This gives a frequency $\kappa/(2\pi) = 9\,\mathrm{Hz}$, which is similar to the observed frequencies. Here we have modelled the artery as a tube open at both ends. It would perhaps be more appropriate to suppose that the tube is open at the proximal end but closed at the distal end to the fluctuating component of the flow. This is equivalent in our model to a tube open at both ends of twice the length, i.e. 1 m. In this case we should predict a natural frequency of about 5 Hz, which is again of the same order as the observed frequencies.

Two questions which immediately arise are: how are such oscillations excited and how strongly are they damped? Influences exciting the oscillations might include the higher-order Fourier components associated with the sharp rise and fall of the ventricular pressure wave form, and the effect of the nonlinearities explored in § 6. The rate of decay in the absence of forcing may be estimated from (6.11) by supposing that $\alpha_1 \neq 0$ but $\phi_F^{[11]} = 0$ and allowing ω to be complex. Then

$$\omega^2 = (1 - 1/\beta)\,\kappa^2, \quad \mathrm{Im}\,\omega = \kappa/(2\tfrac{3}{2}\alpha).$$

Thus unforced oscillations with frequency $\mathrm{Re}\,\omega \cong \kappa$ are decreased by a factor $\exp[-\pi/(2\frac{1}{2}\alpha)]$ in each cycle. The value of α for a frequency of 5 Hz, vessel radius of 0·6 cm and kinematic viscosity of $0{\cdot}0346\,\mathrm{cm^2/s}$ is $\alpha = 18$ so $\exp[-\pi/(2\frac{1}{2}\alpha)] = 0{\cdot}88$, and oscillations of this frequency could persist throughout the cardiac cycle, assuming a cardiac frequency of about 1 Hz. Persistence for at least half a cycle has frequently been observed in horses.

To conclude, we consider what features our model shares with the real coronary artery. In reality, any disturbance in a blood vessel must propagate as a wave, and

only if its wavelength is much greater than the length of the vessel will the wall motion be independent of axial distance. For a wave with the cardiac frequency, say 1 Hz in the horse, this will be reasonable as then the wavelength, using our estimate for the wave speed of $c = 8\,\mathrm{m/s}$, is about 8 m, compared with a vessel length of 0·5 m. For a fluctuation with frequency 5 Hz the wavelength is about 1·6 m so our assumption is not a good approximation. However one can envisage a situation in which all points on the wall move with the same phase, as in our model, although not all with the same amplitude. This may occur if a standing wave is set up in the vessel, or approximately, if the wave contains a strong reflected component.

Suppose then that our model approximates qualitatively some features of the real flow. We have seen that it predicts the possibility of flow fluctuation with frequency and damping rates consistent with experimental observations. From our model we are also able to predict the nature of the steady-streaming component of the flow. This is likely to be important in determining mass transport in the vessel. It should be noted that, as there is no second-order steady interaction between different frequencies, the steady flows driven by different Fourier components of the pressure fluctuations may be superimposed at second order. At the cardiac frequency (1 Hz), $\alpha \cong 8$ and the steady streaming is small in the centre of the vessel but everywhere directed towards the wall. At frequencies of about 5–10 Hz, $\alpha \cong 20$, so the flow is directed inwards in the core but towards the wall in a fairly thin boundary layer. To obtain a sample value of ϵ, we use figure 1 (*b*) of Rumberger & Nerem (1977). This shows fluctuations of amplitude 4 $\mathrm{cm^3/s}$ peak to peak in the flow rate, with frequency about 7 Hz. The value of ϵ estimated from the volume fluctuations divided by total vessel volume is then of order $\epsilon = 10^{-2}$, so that the low R_s regime applies.

I am grateful to Dr T. J. Pedley for suggesting the problem and for much valuable advice. I acknowledge the receipt of an Overseas Scholarship from the Royal Commission for the Exhibition of 1851.

Appendix. The problem in axisymmetric geometry

In the axisymmetric case, the equations of motion (2.2)–(2.6) become

$$u_t + uu_x + vu_r = -\phi_x + \nu(u_{xx} + r^{-1}(ru_r)_r), \tag{A 1}$$

$$v_t + uv_x + vv_r = -\phi_r + \nu(v_{xx} + r^{-1}(rv_r)_r - r^{-2}v), \tag{A 2}$$

$$u_x + r^{-1}(rv)_r = 0, \tag{A 3}$$

$$u = 0, \quad v = \dot{a} \quad \text{at} \quad r = a. \tag{A 4}$$

The solution to (A 1)–(A 4) in the inviscid case is found to be

$$u = a^2\left\{\int \frac{G(t)}{a^2}\,dt + P(r/a)\right\} - 2\dot{a}x/a,$$

$$v = \dot{a}r/a,$$

$$\phi = \phi_c(t) - \tfrac{1}{2}\ddot{a}r^2/a - G(t)\,x + (\ddot{a}/a - 3\dot{a}^2/a^2)\,x^2,$$

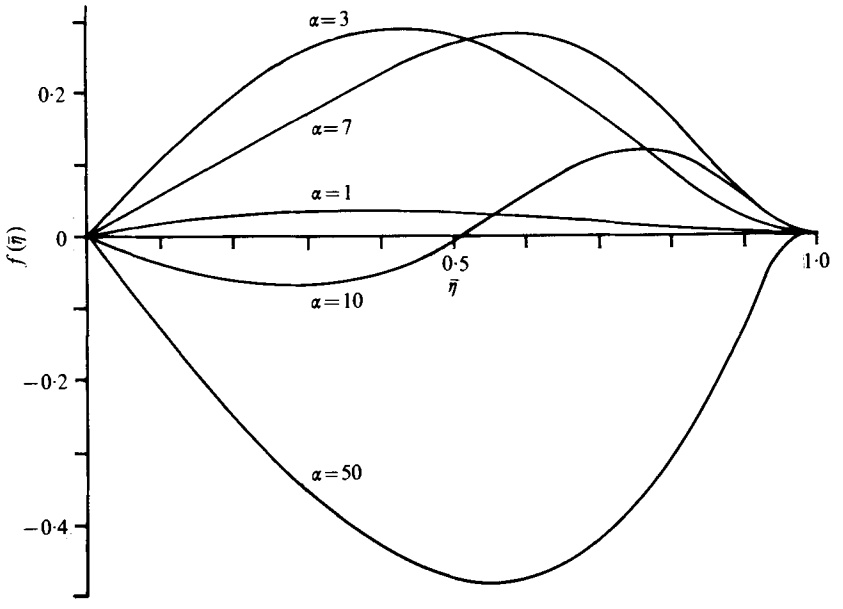

FIGURE 5. The Lagrangian mean streaming velocity in axisymmetric geometry [equation (A 8)].

where ϕ_c, G and P are again unknown functions. Putting $\eta = r/a$, we obtain equations corresponding to (2.12), (2.14) and (2.17):

$$u_{1t} + u_1^2 + (v - \dot{a}\eta)\, a^{-1} u_{1\eta} = -2\phi_2 + \nu a^{-2}\eta^{-1}(\eta u_{1\eta})_\eta; \tag{A 5}$$

$$u_1 + a^{-1}\eta^{-1}(\eta v)_\eta = 0; \tag{A 6}$$

$$u_1 = 0, \quad v = \dot{a} \quad \text{at} \quad \eta = 1. \tag{A 7}$$

We omit the small α solution, which differs from (3.2)–(3.4) only in the values of numerical constants. The solution at small R_s corresponding to (4.3)–(4.5) is found to be

$$\phi_2^{[11]} = -\omega^2 I_0(\beta)/D,$$
$$u_1^{[11]} = -2i\omega(I_0(\beta) - I_0(\beta\eta))/D,$$
$$v^{[11]} = ia_0\omega(\eta I_0(\beta) - 2I_1(\beta\eta)/\beta)/D,$$

where $\beta = \alpha e^{\frac{1}{4}i\pi}$, $D = I_0(\beta) - 2I_1(\beta)/\beta$ and I_0 and I_1 are modified Bessel functions. At second order, we find for the steady components

$$v_L = \omega a_0 f(\bar{\eta}), \quad u_{1L} = -\omega\bar{\eta}^{-1}(\bar{\eta}f)',$$

where

$$f(\bar{\eta}) = \frac{1}{DD^*}\left\{\left(\frac{4}{\beta} I_0(\beta)\, I_1(\beta^*) + \text{c.c.} - \tfrac{3}{2} I_1(\beta)\, I_1(\beta^*)\right)(2\bar{\eta} - \bar{\eta}^3)\right.$$
$$- \tfrac{1}{2}\bar{\eta}\left[I_1(\beta\bar{\eta})\, I_1(\beta^*\bar{\eta}) + 2I_1(\beta)\, I_1(\beta^*) - \left(\beta^* \int_{-1}^{\eta} I_1(\beta\eta)\, I_0(\beta^*\eta) + \text{c.c.}\right)\right]$$
$$\left. - \left(\frac{1}{\beta^*} I_1(\beta\eta)\,(3I_0(\beta^*) + I_0(\beta^*\eta)) + \text{c.c.}\right)\right\}. \tag{A 8}$$

The function f is plotted in figure 5 for several values of α.

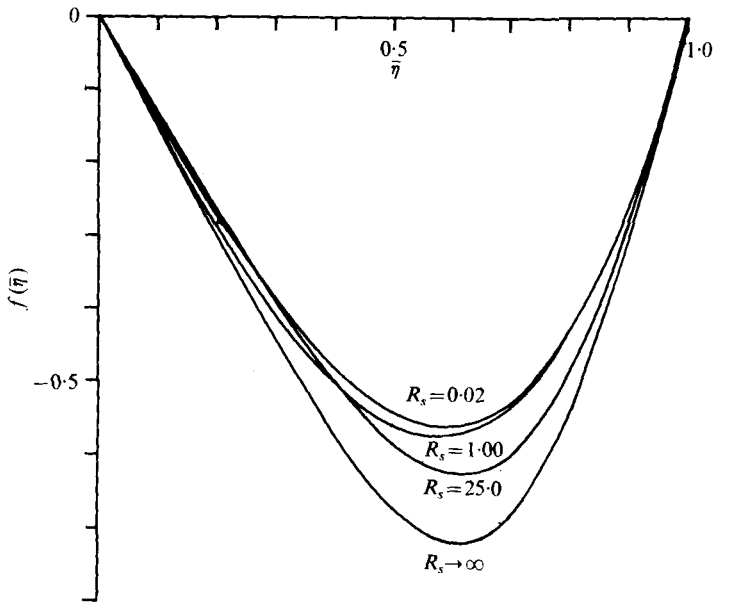

FIGURE 6. The steady streaming velocity in the core in axisymmetric geometry for large α, from (A 11) (R_s finite) and (A 14) ($R_s\to\infty$).

We now consider the problem at large α and at moderate and large values of R_s. From (A 5) and (A 6),

$$a^{-1}\eta^{-1}(\eta v_t)_\eta - \dot{a}a^{-2}\eta^{-1}(\eta v)_\eta - a^{-2}\eta^{-2}((\eta v)_\eta)^2 + a^{-2}(v-\dot{a}\eta)\,(\eta^{-1}(\eta v)_\eta)_\eta$$
$$= 2\phi_2 + \nu a^{-3}\eta^{-1}(\eta(\eta^{-1}(\eta v)_\eta)_\eta)_\eta.$$

Setting $v = \dot{a}\eta + a^5 F(\eta, t)$ we obtain

$$F_{\eta t} + \eta^{-1}F_t + a^4(FF_{\eta\eta} - F_\eta^2 - \eta^{-1}FF_\eta - 2\eta^{-2}F^2)$$
$$= 2a^{-4}\bar{\phi}_2 + \nu a^{-2}(F_{\eta\eta\eta} + 2\eta^{-1}F_{\eta\eta} - \eta^{-2}F_\eta + \eta^{-3}F), \qquad \text{(A 9)}$$

where $$\bar{\phi}_2 = \phi_2 - \ddot{a}/a + 3\dot{a}^2/a^2.$$

Applying the method of matched asymptotic expansions to cases (i) and (ii), as in § 5, and setting

$$v_L = a_0^5 F^{[20]} = a_0\,\omega f(\eta)$$

and $$f(\eta) = \tau^{-\frac{1}{2}}g(\tau), \quad \text{where} \quad \tau = \eta^2, \qquad \text{(A 10)}$$

we obtain

(i) $$gg'' - g'^2 = \tfrac{1}{4}K + 2N^{-2}(\tau g''' + g''), \qquad \text{(A 11)}$$

(ii) $$gg'' - g'^2 = \tfrac{1}{4}K, \qquad \text{(A 12)}$$

with in both cases $$g(\tau) = o(\tau^{\frac{1}{2}}) \text{ as } \tau\to 0, \quad g(1) = 0, \quad g'(1) = \tfrac{3}{2}. \qquad \text{(A 13)}$$

In case (ii) we find that solutions are given by

$$g = (-1)^n \frac{3}{2n\pi}\sin n\pi\tau,$$

i.e.
$$f(\eta) = (-1)^n \frac{3}{2n\pi} \frac{\sin n\pi\eta^2}{\eta}.$$

The same argument as was used in § 5 shows that

$$f(\eta) = -\frac{3}{2\pi} \frac{\sin \pi\eta^2}{\eta}. \tag{A 14}$$

In case (i), numerical methods are required. Equation (A 11) is singular at the origin so a power-series solution was used on the interval [0, 0·1] and the unknown parameters obtained by matching with a numerical solution for the interval [0·1, 1]. Figure 6 shows the function $f(\eta)$ at several different values of R_s, along with the solution (A 14) of case (ii).

The problem of an elastically constrained wall in axisymmetric geometry follows the same lines as the two-dimensional problem. In the inviscid case,

$$\phi_2 = \ddot{a}/a - 3\dot{a}^2/a^2, \tag{A 15}$$

so
$$\ddot{a}/a - 3\dot{a}^2/a^2 + 6f(a)/L^2 = 6\phi_F/L^2. \tag{A 16}$$

An equation similar to (6.5) results from setting $s = a_0^2/a^2$, and if one takes

$$f(a) = k(a^2 - a_0^2),$$

(6.6) is again obtained. For small oscillations about $a = a_0$ the natural frequency κ is given by

$$\kappa^2 = 6a_0 f'(a_0)/L^2. \tag{A 17}$$

REFERENCES

Abramowitz, M. & Stegun, I. A. (eds) 1965 *Handbook of Mathematical Functions*. Dover.

Batchelor, G. K. 1967 *An Introduction to Fluid Mechanics*. Cambridge University Press.

Longuet-Higgins, M. S. 1953 Mass transport in water waves. *Phil. Trans. Roy. Soc.* A **245**, 535.

Nerem, R. M., Rumberger, J. A., Gross, D. R., Muir, W. W. & Geiger, G. L. 1976 Hot-film coronary artery velocity measurements in horses. *Cardiovasc. Res.* **10**, 301.

Proudman, I. 1960 An example of steady laminar flow at large Reynolds number. *J. Fluid Mech.* **9**, 593.

Rayleigh, Lord 1884 On the circulation of air observed in Kundt's tubes, and on some allied acoustical problems. *Phil. Trans. Roy. Soc.* A **175**, 1.

Riley, N. 1965 Oscillating viscous flows. *Mathematika* **12**, 161.

Riley, N. 1967 Oscillatory viscous flows. Review and extension. *J. Inst. Math. Appl.* **3**, 419.

Rumberger, J. A. & Nerem, R. M. 1977 A method-of-characteristics calculation of coronary blood flow. *J. Fluid Mech.* **82**, 429.

Stuart, J. T. 1963 Unsteady boundary layers. In *Laminar Boundary Layers* (ed. L. Rosenhead), p. 349. Oxford: Clarendon Press.

Stuart, J. T. 1966 Double boundary layers in oscillatory viscous flow. *J. Fluid Mech.* **24**, 673.

Uchida, S. & Aoki, I. 1977 Unsteady flows in a semi-infinite contracting or expanding pipe. *J. Fluid Mech.* **82**, 371.

Wells, M. K., Winter, D. C., Nelson, A. W. & McCarthy, T. C. 1974 Hemodynamic patterns in coronary arteries. In *Fluid Dynamic Aspects of Arterial Disease* (ed. R. M. Nerem), p. 36. Ohio State University.